Enhancing deep pre-carbonate imaging with DAS VSP mode-converted energy: Unlocking deeper exploration potential in the prolific Asia Pacific basins

Riaz Alai[1], Ahmad Riza Ghazali[1], Faizan Akasyah Ghazali[1], Ming Heng Pua[1], Edysuzaily B Kamarudin[1], Garry B Malo-Paul[1], Hasnor Farhana Hasnan[1], Gundogan Coskun[1], Yusliza Bt M Sufian[1], Sandeep Kumar[1], Mohamad Rizam Sarif[1], Khairul Hamidi B Khalid[1], Mitch Preston[2], Shuqian Dong[2], Ge Zhan[2], Faqi Liu[2], Rachel Collings[2], Simon Shaw[3], and Oscar Barrios-Lopez[3]

https://doi.org/10.1190/tle-2025-1023

Abstract

The South Asia region hosts multiple prolific play types in its Tertiary basins. It is common to see cycles of carbonates and siliciclastic reservoir targets distributed from very shallow levels to deep early basin fills. The presence of thick, high-impedance carbonate layers with highly variable geometry at mid-section poses significant challenges for imaging productive deeper target levels. Over the years, numerous studies have explored methods to enhance pre-carbonate imaging, from acquisition strategies to the application of specialized technologies during seismic data processing. Here, mode conversions at the high-impedance contrast interfaces of these carbonate layers were explored and used in improving imaging of the target sections. In a shallow-water survey in the Asia Pacific region, surface data (marine and ocean-bottom node) and borehole data (3-component vertical incidence vertical seismic profiling [VSP] and 3D distributed acoustic sensing [DAS] VSP) were acquired to advance subsurface imaging. In standard DAS VSP data processing workflows, energy not associated with primary P-waves is often attenuated or removed as noise. In contrast, the importance of this noise, comprising mode-converted and multiple energy, was highlighted, as it played a critical role in improved pre-carbonate imaging. Imaging using this mode-converted and multiple energy was shown to have great potential to provide additional insight into the reservoir structures beneath the shallow carbonates. A 3D VSP survey using a wireline fiber-optic cable was conducted in a deviated well. Despite the single-component limitation of DAS recording, the acquired 3D DAS VSP data captured P-waves and notable converted waves, resulting from mode conversions within a shallow, high-velocity carbonate layer. This paper highlighted key findings from the analysis of the 3D DAS VSP data and examined the possibility of using converted waves and multiple energy for DAS VSP deeper carbonate imaging in a geologically complex setting.

Introduction

Seismic imaging in complex carbonate settings, particularly in shallow-water environments, remains highly challenging. These difficulties originate from a complex overburden dominated by a shallow, high-velocity carbonate layer with strong acoustic impedance contrasts. As a result, conventional surface seismic data often produce poor-quality images with limited continuity of subsurface reflectors. To address these limitations and improve the imaging fidelity, four complementary data sets were acquired: marine streamer data for initial velocity model building and broad coverage, an ocean-bottom node (OBN) configuration to enhance the low-frequency content and accommodate full-azimuth illumination, a 3-component vertical incidence vertical seismic profiling (3-C VIVSP) for anisotropy analysis and high-resolution borehole imaging, and 3D distributed acoustic sensing (DAS) VSP data for dense spatio-temporal sampling and improved vertical resolution. This integrated acquisition strategy was designed to address imaging challenges and to enable advanced processing workflows such as elastic inversion, reverse time migration (RTM), and high-fidelity reservoir characterization (see Figure 1).

Figure 2 [left] shows a perspective view of the surface shot locations (in red) and the geometry of the downhole fiber-optic cable used in the 3D DAS VSP (in blue and orange). A reservoir horizon is also highlighted in yellow within the same plot. The data acquisition covered a source patch measuring 8 km × 8 km, with a shot spacing of 50 m × 50 m, resulting in a total of 24,400 shot points. Figure 2 [right] presents six raw DAS VSP shot gathers sampled at various offsets along a single-shot line (the source locations are indicated by green dots in Figure 2 [left]). These field records demonstrate DAS VSP data with a reasonably good signal-to-noise ratio, despite being acquired using wireline fiber, which is known for suboptimal coupling. Additionally, it was observed that the

Manuscript received 2 September 2025; revision received 22 October 2025; accepted 3 November 2025.

[1]PETRONAS Carigali Sdn. Bhd., Kuala Lumpur, Malaysia. E-mail: riaz.alai@petronas.com; rizag@petronas.com; faizan_akasyah@petronas.com; pua.mingheng@petronas.com; edysuzaily_kamarudin@petronas.com; garrymalo@petronas.com; farhana.hasnan@petronas.com; gundogan.coskun@petronas.com; yusliza_s@petronas.com; sandeepkumar@petronas.com; mrizam.sarif@petronas.com; hamidik@petronas.com.

[2]TGS, Houston, Texas, USA. E-mail: mitch.preston@tgs.com; shuqian.dong@tgs.com; ge.zhan@tgs.com; faqi.liu@tgs.com; rachel.collings@tgs.com.

[3]Halliburton, Houston, Texas, USA. E-mail: simon.shaw@halliburton.com; oscaraugusto.barrios@halliburton.com.

upgoing P-wave (P-Up) signal for shots located opposite to the well deviation is weak, and in some cases absent, due to the inherent fiber directivity in DAS acquisition, whereas the upgoing P-to-S converted wave (PS-Up) signal can be strongest for these shots.

DAS used for VSP has emerged as a transformative tool for subsurface characterization, using existing fiber-optic cables as dense seismic arrays to deliver high-resolution imaging without geophones (Mateeva et al., 2012). This approach reduces costs, broadens monitoring accessibility, and has proven effective in exploration and carbon storage projects. Studies highlight its scalability across diverse geologic settings, including time-lapse monitoring to track subtle subsurface changes (Daley et al., 2013). Recent advances in full-waveform inversion (FWI) and imaging workflows further enhance resolution and velocity model building (Liu et al., 2025Zhan et al., 2024). Multiwell surveys with preinstalled fiber-optic cables extend subsurface illumination beyond the borehole (Zhan and Nahm, 2020), and the integration of surface and borehole data enables true-3D imaging beneath complex overburdens (Ghazali et al., 2018). Recent advances in processing techniques include the use of deep learning for denoising and wavefield separation (Cheng et al., 2025). All these developments position 3D DAS VSP as a versatile and increasingly mature technology with significant geophysical applications.

Alai et al. (2024) challenge conventional imaging approaches in complex carbonate environments by integrating mode-converted shear waves and electromagnetic data to reduce interpretational ambiguity and enhance subsurface characterization. Alai et al. (2025) demonstrate the value of imaging shear waves in carbonate environments identified from DAS VSP data.

Figure 3 illustrates the comparison of VIVSP shots recorded using geophones and DAS. Note the interesting similarities observed in both displays. For the DAS VSP data, selective source–receiver extractions have been made to match the source–receiver Walkabove VSP configuration for optimal comparison of both VSP data. The analysis of the recorded DAS VSP data revealed essential acoustic-to-elastic wave mode conversions at the carbonate layer.

To better understand the mode-converted energy in DAS VSP data, elastic finite-difference modeling was performed. Figure 4a shows a complex overburden (the velocity model was estimated from the streamer data), dominated by a shallow, high-velocity carbonate layer with significant acoustic impedance. Figure 4b shows a snapshot of mode conversions obtained using constant-density elastic forward numerical modeling. A linear V_P–V_S relationship was derived from the compressional- and shear-sonic logs via least-squares regression, ensuring the best agreement between estimated and observed V_S, and then applied to the streamer 3D V_P model (Figure 4a) to obtain the V_S model.

Figure 4c and 4d shows the comparison of elastic modeled and field data, emphasizing their similarities and confirming that downgoing P-waves undergo multiple mode conversions at the top of carbonate (TOC) and base of carbonate (BOC), generating prominent P-to-S converted waves.

These converted waves significantly interfere with P-waves, posing challenges for conventional VSP imaging that relies on P-wave data only. On the other hand, because mode-converted waves are dominant over P-waves, they provide additional insight into pre-carbonate imaging.

VSP wavefield separation and shear velocity estimation

As shown in Figures 1–4, the DAS VSP data show a reasonably good signal-to-noise ratio, despite being acquired using wireline fiber.

Imaging VSP converted waves requires isolating the upgoing converted wavefield from the full wavefield, making wavefield separation a critical step in the processing workflow. In this paper, the separation was performed in two stages: the full wavefield was separated into upgoing and downgoing components using a dip-separation-based approach.

In addition, the upgoing wavefield was decomposed into upgoing PP- and PS-wave components based on their moveout characteristics (Figure 5a [left] and [center]). Ray-tracing-based moveout correction was applied to flatten the upgoing P-wave events in the shot domain, after which P-wave energy was separated from the PS signal via curvelet-domain filtering. Figure 5a [right] presents a color-coded integrated display of the upgoing S-waves (red) overlaid on the upgoing P-waves (blue), highlighting that the upgoing S-waves are more prominent

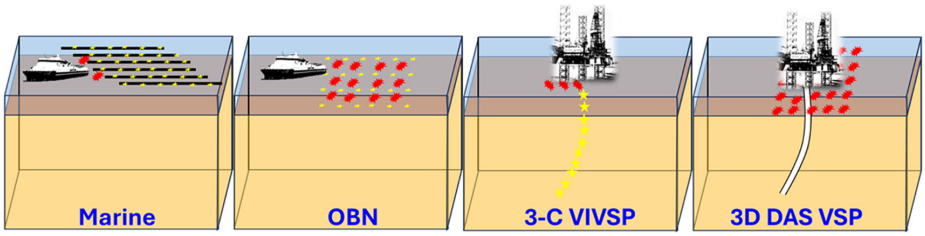

Figure 1. Different acquisition types (from left to right): marine streamer data, OBN data, 3-C VIVSP data, and 3D DAS VSP data.

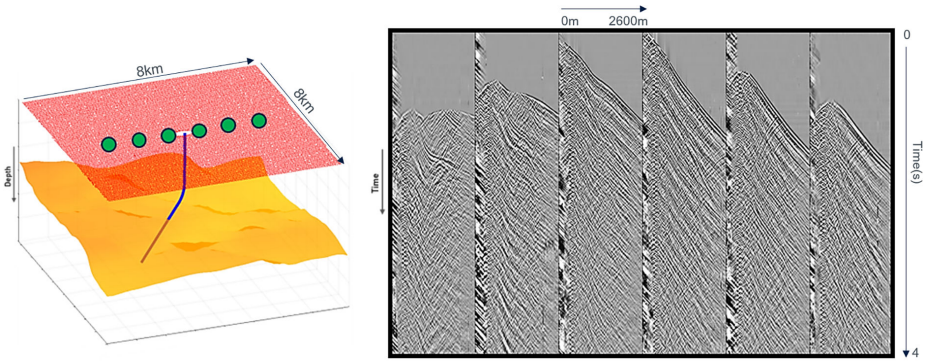

Figure 2. A 3D view of the acquisition geometry and display of six field DAS VSP shot gathers at various offsets. The green dots indicate the source locations.

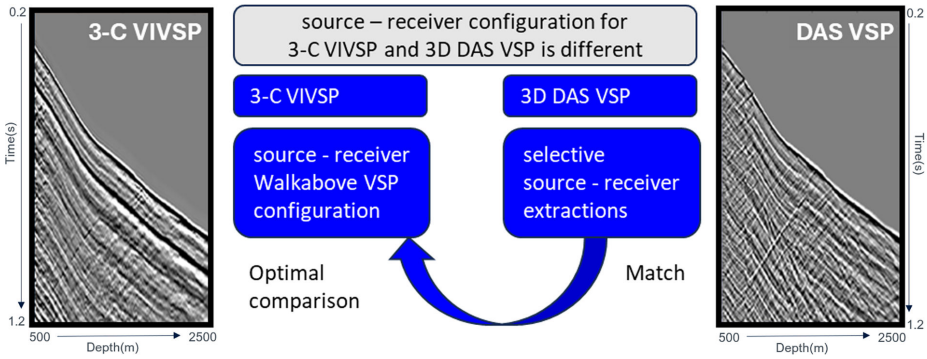

Figure 3. Comparison of VIVSP shots recorded using geophones and DAS: vertical component of geophone VSP data [left] and DAS VSP data [right]. For the DAS VSP, selective source–receiver extractions have been made to match the source–receiver Walkabove VSP configuration for optimal comparison of both VSP data.

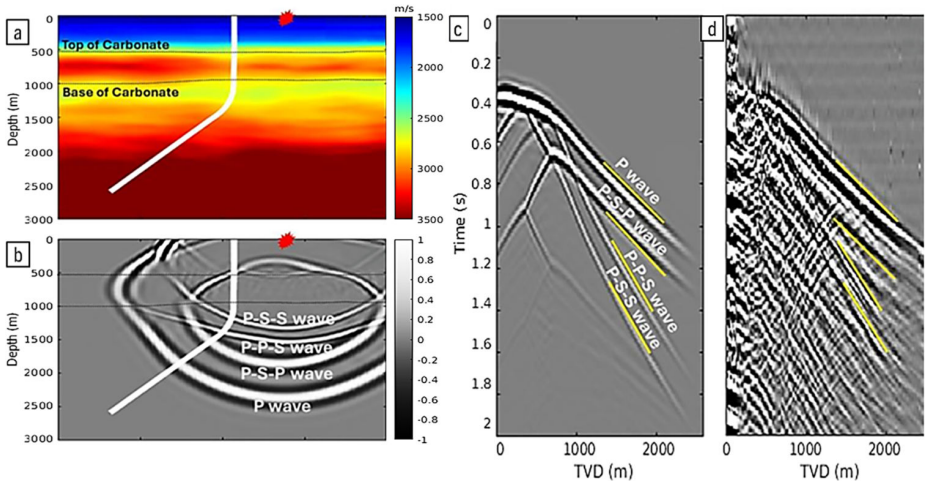

Figure 4. Wave mode conversions with P-waves propagating through a carbonate layer: (a) P-wave velocity model, with the red dot indicating the surface shot location and the white line representing the fiber-optic cable; (b) snapshot of the elastic wavefield, highlighting multiple mode conversions at the carbonate layer; (c) synthetic modeled VSP; and (d) DAS VSP.

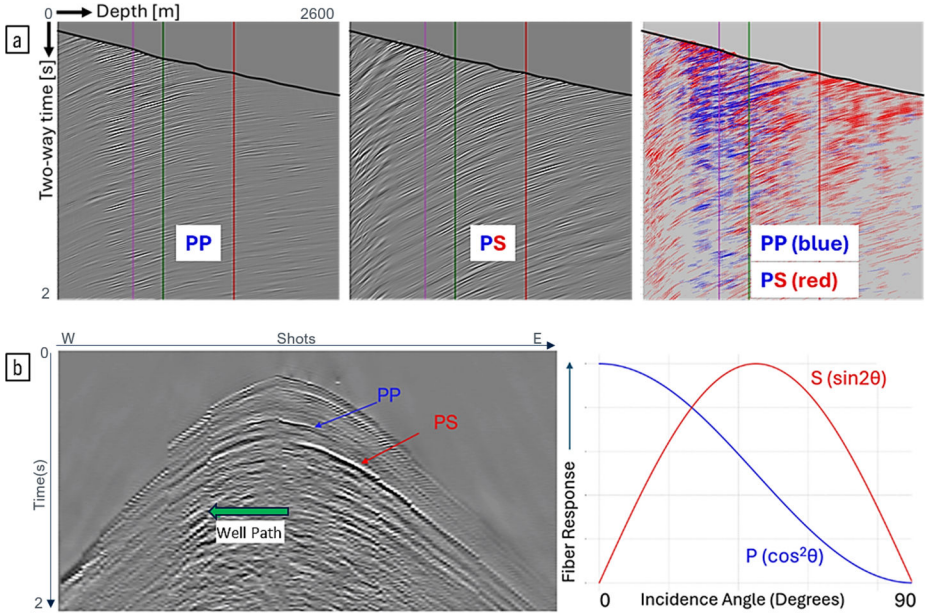

Figure 5. Upgoing waves in DAS VSP data: (a) from left to right: PP waves, PS waves, and integrated display of PS waves (red) overlaid on PP waves (blue). (b) DAS VSP channel gather showcasing PP versus PS signal dominance on a sail line parallel to the well path [left] and plot of theoretical fiber response to P ($\cos^2\theta$) and S ($\sin 2\theta$) waves [right].

than the upgoing P-waves, particularly in the deeper deviated section of the fiber.

The recorded amplitude in DAS depends on the incidence angle θ between the incoming wavefield and the fiber axis. The P-wave response scales as $\cos^2\theta$ (blue curve, Figure 5b [right]): it is maximum for waves parallel to the fiber (θ = 0°) and decreases toward zero at 90°. The shear-wave response scales as $\sin 2\theta$ (red curve, Figure 5b [right]), vanishing at 0° and 90° and peaking at 45°. The S response exceeds the P response for θ > 26.6° (where $\cos^2\theta = \sin 2\theta$). This trend appears in the channel gather from the deviated section (Figure 5b [left]). There is a clear transition where the P-wave energy diminishes, whereas PS energy strengthens and becomes dominant energy in the record.

For improved understanding of the acquired DAS VSP data, Figure 6 shows the recordings for a source offset of 1500 m. Note the shallow water multiples: the P-wave interbed multiples bouncing between water bottom (WB) and TOC and the P-wave and S-wave interbed multiples bouncing between the TOC and BOC. It is noted that the mode-converted S-waves are dominant (indicated with the red arrows) in the pre-carbonate section.

It is interesting to observe the interbed multiples generated at the BOC: the wave propagation and reflections colored indicate P-wave (blue) and S-wave (red) interbed multiples generated at the BOC. This important finding emphasizes that using P-waves alone makes it very challenging to obtain high-quality and accurate actual pre-carbonate images.

The DAS VSP data were obtained to improve the mapping of geologic structures and deliver more accurate insights into the VSP well, especially for characterizing reservoirs beneath the shallow carbonate layer. As emphasized above, in early stages of processing DAS VSP data, all signals not associated with P-waves are

typically eliminated from the data. In this paper, we recommend retaining these; however, for illustrative purposes, we present the following example. Figure 7a shows three shots parallel to the well path, full wavefield (grayscale), input to FWI after PS attenuation (blue). To achieve these gathers, forward elastic numerical modeling was performed to accurately model all mode-converted energy followed by the removal of all of these from the shot gathers. Figure 7b illustrates the cross-correlation maps of the direct arrival between field and synthetic data modeled using acoustic engine for FWI updates (from left to right): starting model, 10, 12, and 15 Hz. Stronger blue and red values represent high mismatch, whereas white represents a good match.

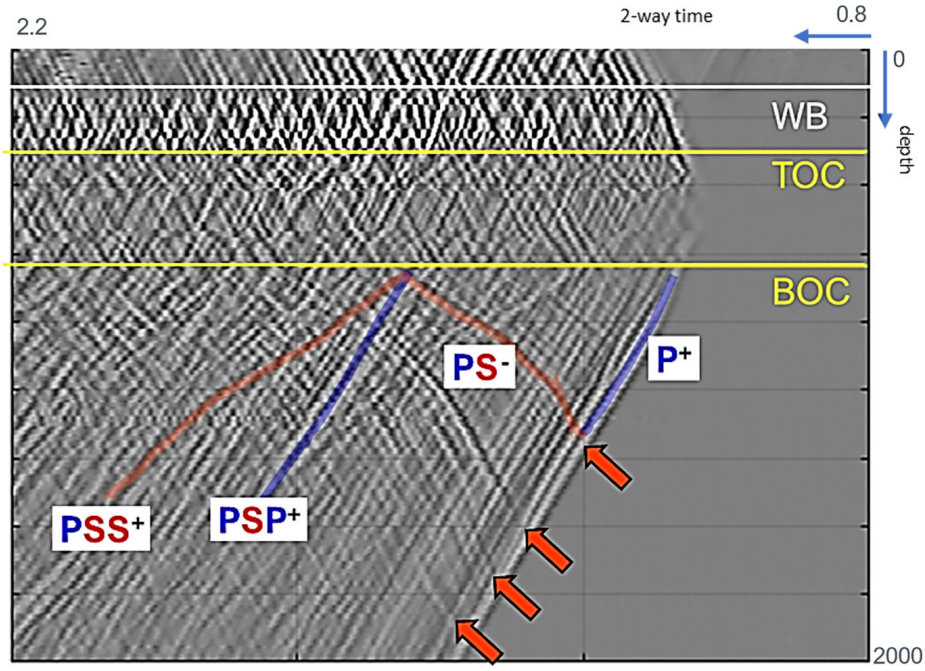

Figure 6. 3D DAS VSP data for a source offset of 1500 m. Note the shallow water multiples: the P-wave interbed multiples bouncing between WB and TOC and the P-wave interbed multiples bouncing between the TOC and BOC. Interestingly, in the pre-carbonate section, mode-converted S-waves are dominant (red arrows). The colored wave propagation and reflections indicate P-wave (blue) and S-wave (red) interbed multiples generated at BOC. This important finding emphasizes that using P-waves alone makes it very challenging to obtain high-quality and accurate deeper pre-carbonate images.

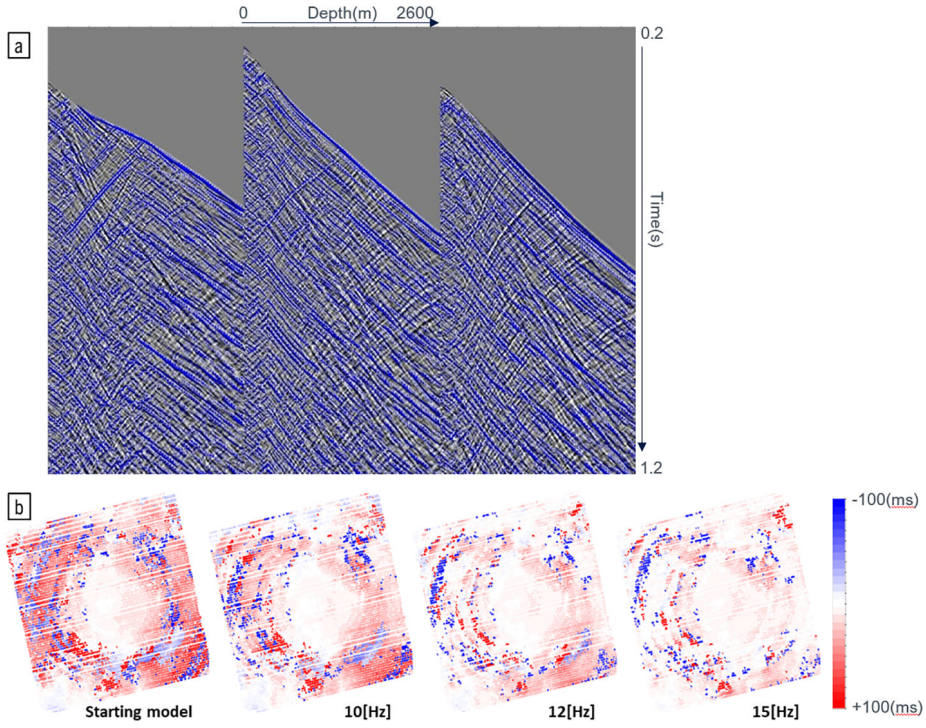

Figure 7. (a) Three shots parallel to the well path, full wavefield (grayscale), input to FWI after PS attenuation (blue). (b) Cross-correlation misfit maps of the direct arrival between field and synthetic acoustic modeling for FWI updates (from left to right): starting model, 10, 12, and 15 Hz. Stronger blue and red values represent high mismatch, whereas white represents a good match.

Converted waves and multiple imaging with RTM

Using the P-wave interval velocity estimated from the acoustic FWI, we first used RTM to generate a P-Up image. Compared with the marine surface-seismic image, the 3D DAS VSP P-Up image shows a broader bandwidth and higher dominant frequencies. This is a typical benefit of VSP acquisition: borehole receivers are closer to the formation, so the upgoing wavefield travels a shorter, less-attenuative path in the subsurface.

Figure 8a shows the comparisons of the DAS VSP P-Up image [left] and DAS VSP PS-Up image [center]. Imaging the primaries shows that the illumination area obtained from using the upgoing wavefields is limited to around the borehole and is not present within the shallow section where no receivers are present. To overcome this, imaging with multiples (Lu et al., 2015), also known as separated wavefield imaging (SWIM), was used to extend the illumination area and obtain an image of the near surface (Figure 8a [right]). SWIM uses each shot as a "virtual" receiver, expanding the surface coverage of the seismic experiment to the shot patch and enhancing the subsurface illumination. This results in a survey that has a spatial sampling richer in offsets and azimuths. The improved spatial sampling greatly enhances the angular diversity of the data at every image point, which results in the imaging of reflectivity above the fiber.

Figure 8b shows the multiple imaging raypath diagrams (from left to right): P-Down direct

arrival, P-Down first-order surface-related multiples, P-Down second-order surface-related multiples, and P-Down higher order surface-related multiples.

A comparison between the streamer seismic Kirchhoff prestack depth migrated (KPSDM) image (Figure 9 [left]) and the 3D DAS VSP multiple image (Figure 9 [center]), and the cross-correlation between them (Figure 9 [right]) shows clearly their similarities between both data sets, with DAS VSP data exposing higher frequency content. Both seismic sections have been stretched to two-way time with their own respective velocities for the cross-correlation applications. All sections have been mapped back to depth for comparison purposes (Figure 10). It should be noted that the imaging of multiples of 3D DAS VSP covers only a certain lateral distance around the well but has significantly contributed to the lateral imaging in comparison with imaging primaries only.

Prior to migrating the upgoing converted waves, a shear model (V_S) was determined using the sonic and shear logs.

The PS imaging input was generated by first aligning the upgoing PS arrivals. We computed PS traveltimes via ray tracing using the P-wave velocity for the downgoing leg and the S-wave velocity for the upgoing leg and applied the resulting dual-velocity moveout to flatten PS events in the shot domain. After flattening, curvelet-domain filtering suppressed PP leakage and incoherent noise.

The upgoing S-waves were migrated using reciprocity with dual-velocity acoustic RTM as proposed by Alai et al. (2022).

In this approach, the forward source propagation is carried out downhole using the constructed S-wave velocity, whereas the upgoing S-wave field is backward propagated from surface shot locations to the subsurface using either the P-wave velocity or various types of converted wave velocities. This process is graphically illustrated in the ray diagrams shown in Figure 11a.

For comparison purposes, the surface seismic PP image (grayscale) and the conventional DAS VSP image of the upgoing P-waves (PPPP) are shown in Figure 11b (left and center, respectively). Note that the VSP images are overlaid in gold color on the surface seismic across the wellbore direction. Figure 11b [right] demonstrates improved imaging of deeper reflectors (indicated by the yellow arrow) using upgoing shear waves (PPPS). Figure 11c shows a schematic ray diagram illustrating some possible mode-converted PSPP, PPPS, and PSPS waves in carbonate settings. These are a subselection of all the possible configurations PPPP, PPSP, PSPP, PSSP, PPSS, PSPS, and PSSS.

Finally, Figure 12 shows the comparison of the KPSDM surface data and DAS VSP RTM images using mode-converted waves. Note the depth coincidence of all the images (indicated with yellow and cyan arrows), even though dual velocities have been used in the RTM. The orange arrows indicate the improved deeper imaging.

The strong alignment between the DAS VSP converted wave images and the surface seismic image demonstrates that this complex carbonate geologic setting is well-suited for using converted waves in DAS VSP imaging. Furthermore,

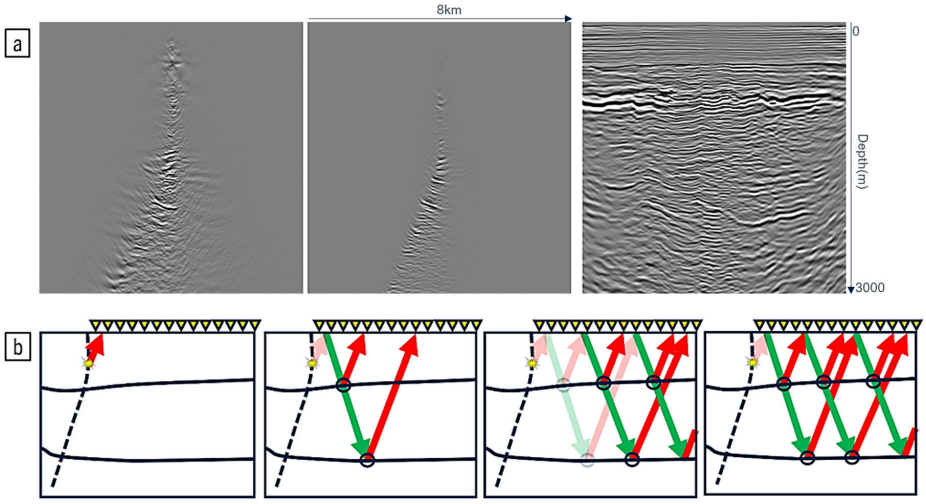

Figure 8. (a) DAS VSP P-Up image [left], DAS VSP PS-Up image [center], and DAS VSP multiple image using all-order surface-related multiples [right]. (b) Multiple imaging raypath diagrams (from left to right): P-Down direct arrival, P-Down first-order surface-related multiples, P-Down second-order surface-related multiples, and P-Down all-order surface-related multiples.

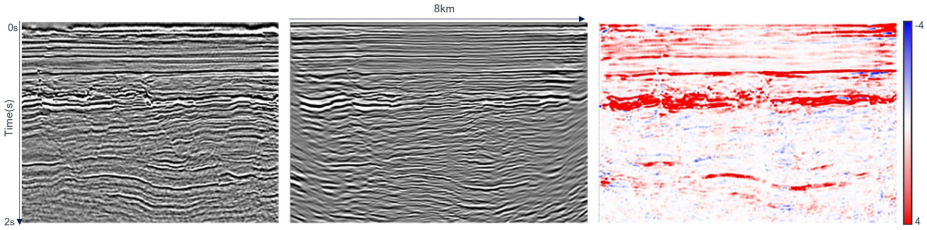

Figure 9. Streamer seismic KPSDM raw image [left], 3D DAS VSP multiple image [center], and cross-correlation between both [right]. Both seismic sections have been stretched to two-way time with their own respective velocities for the cross-correlation applications.

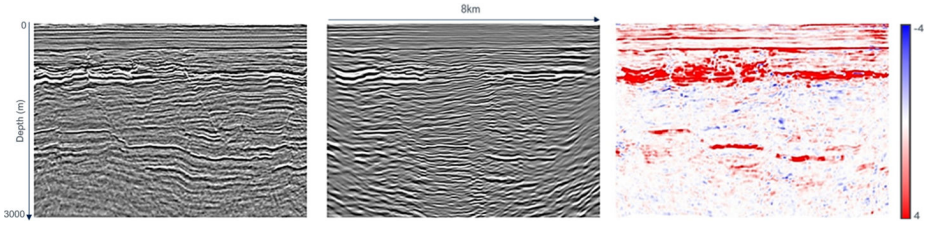

Figure 10. Streamer seismic KPSDM raw image [left], 3D DAS VSP multiple image [center], and cross-correlation between both [right]. Both seismic sections have been stretched to two-way time with their own respective velocities for the cross-correlation applications, and all sections have been mapped back to depth for comparison purposes.

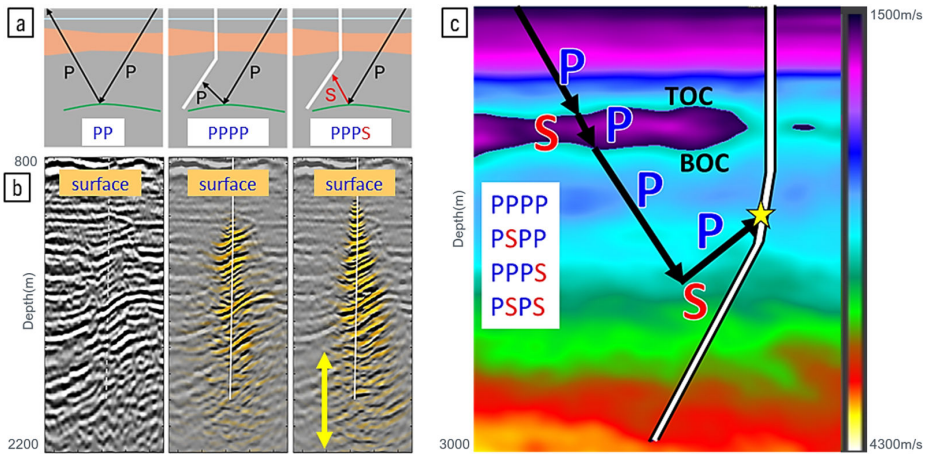

Figure 11. (a) Composite plot with ray diagrams, (b) surface seismic image (grayscale) and DAS VSP PPPP and PPPS images (gold) overlaid on surface seismic across wellbore direction, and (c) schematic diagram illustrating possible mode-converted PSPP, PPPS, and PSPS waves in carbonate settings with the TOC and BOC. Only a subselection of all the possible configurations PPPP, PPSP, PSPP, PSSP, PPSS, PSPS, and PSSS is shown.

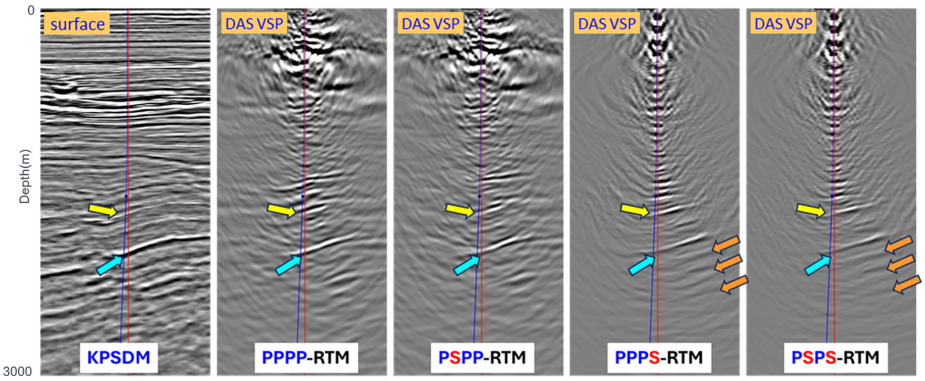

Figure 12. Comparisons of migrated images (from left to right): KPSDM, PPPP RTM, PSPP RTM, PPPS RTM, and PSPS RTM. Note the depth coincidence of all images (yellow and cyan arrows), even though dual velocities have been used in the RTM. Orange arrows indicate improved deeper imaging.

the DAS VSP converted wave images provide subsurface imaging comparable to the conventional P-wave images while also resolving additional features that complement the P-wave only images.

Conclusions

This paper introduces an innovative seismic imaging approach for complex carbonate environments by leveraging converted waves and multiple energy from DAS VSP data. Unlike conventional methods that rely heavily on P-wave data and often struggle beneath high-velocity carbonate layers, this study successfully used converted S-waves and multiples to improve subsurface resolution. The 3D DAS VSP data were acquired using a wireline-deployed fiber-optic cable in a shallow water setting, demonstrating the feasibility and effectiveness of this technique.

Rather than following industry standard routinely removing nonprimary-P-wave energy as noise in DAS VSP data, this paper demonstrated that these mode-converted waves and multiple energy can be used in deeper pre-carbonate imaging, opening deeper exploration opportunities. We imaged mode-converted energy to extract valuable information. Our analyses have provided critical insights into acoustic-to-elastic mode-converted waves within and beneath the carbonate layers.

The resulting images clearly demonstrate improvement in comparison to surface seismic and conventional DAS VSP upgoing P-wave images in the vicinity of the well.

Our success in imaging mode-converted energy in 3D DAS VSP data establishes a novel foundation for advanced elastic wavefield analyses in complex carbonate geologic settings.

Future processing of the OBN data and integration with the 3D DAS VSP may provide more accurate shear interval velocities. With joint updates of P- and S-wave interval velocities, full elastic RTM needs to be performed to achieve optimal results taking all elastic boundary conditions into account. TLE

Acknowledgments

The authors thank PETRONAS Management for the support and permission to publish the results. We thank TGS and Halliburton for the collaboration efforts.

Data and Materials Availability

PETRONAS is owner of the data. Therefore the data can not be released.

Corresponding author: riaz.alai@petronas.com

References

Alai, R., A. R. Ghazali, F. A. Ghazali, P. M. Heng, E. Kamarudin, M. Preston, S. Dong, et al., 2025, Insights from DAS VSP converted wave imaging in complex carbonate geological settings: Fifth International Meeting for Applied Geoscience & Energy, SEG/AAPG, Expanded Abstracts.

Alai, R., A. R. Ghazali, L. MacGregor, F. A. Ghazali, E. Kamarudin, A. H. Azmi, G. Malo-Paul, et al., 2024, Challenging preconceptions in complex carbonate imaging: Using shear waves and electromagnetic data for improved subsurface understanding: Fourth International Meeting for Applied Geoscience & Energy, SEG/AAPG, Expanded Abstracts, 587–591, https://doi.org/10.1190/image2024-4101222.1.

Alai, R., F. Liu, D. Armentrout, D. Brookes, T. Johnson, M. Cvetkovic, G. Coskun, et al., 2022, Improved subsalt imaging in Brazil Campos basin - cascaded application of hybrid interbed demultiple, P- and S-salt velocity joint migration, and subsalt converted wave

suppression: Second International Meeting for Applied Geoscience & Energy, SEG/AAPG, Expanded Abstracts, 2680–2684, https://doi.org/10.1190/image2022-3740399.1.

Cheng, M., J. Lin, X. Dong, and T. Zhong, 2025, A multitask deep-learning model for the denoising, interpolation, and wavefield separation of distributed acoustic sensing-vertical seismic profiling data: Geophysics, **90**, no. 6, V559–V568, https://doi.org/10.1190/geo2024-0531.1.

Daley, T. M., B. M. Freifeld, J. Ajo-Franklin, S. Dou, R. Pevzner, V. Shulakova, S. Kashikar, et al., 2013, Field testing of fiber-optic distributed acoustic sensing (DAS) for subsurface seismic monitoring: The Leading Edge, **32**, no. 6, 699–706, https://doi.org/10.1190/tle32060699.1.

Ghazali, A. R., N. ElKady, M. F. Abd Rahim, R. J. J. Hardy, F. S. Dzulkelfi, S. Chandola, S. Kumar, et al., 2018, Reservoir delineation beneath a heterogeneous shallow gas overburden using 'True-3D' seismic imaging approaches: First Break, **36**, no. 11, 89–96, https://doi.org/10.3997/1365-2397.n0137.

Liu, F., C. Macesanu, H. Xing, M. Romanenko, G. Zhan, C. Calderón-Macías, and B. Wang, 2025, Elastic full-waveform inversion: Enhance imaging for legacy and modern acquisition: The Leading Edge, **44**, no. 5, 338–343, https://doi.org/10.1190/tle44050338.1.

Lu, S., D. N. Whitmore, A. A. Valenciano, and N. Chemingui, 2015, Separated-wavefield imaging using primary and multiple energy: The Leading Edge, **34**, no. 7, 770–778, https://doi.org/10.1190/tle34070770.1.

Mateeva, A., J. Mestayer, B. Cox, D. Kiyashchenko, P. Wills, J. Lopez, S. Grandi, et al., 2012, Advances in distributed acoustic densing (DAS) for VSP: 82nd Annual International Meeting, SEG, Expanded Abstracts, 1–5, https://doi.org/10.1190/segam2012-0739.1.

Zhan, G., F. Gao, R. Malik, M. Preston, C. Macesanu, H. Hu, C. Calderón, et al., 2024, Optimizing DAS VSP value through FWI imaging: 85th EAGE Annual Conference & Exhibition, 1–5, https://doi.org/10.3997/2214-4609.202410927.

Zhan, G., and J. Nahm, 2020, Multi-well 3D DAS VSPs: Illumination and imaging beyond the wellbores: 90th Annual International Meeting, SEG, Expanded Abstracts, 3798–3802, https://doi.org/10.1190/segam2020-3426032.1.